J. Electrochem. Sci. Eng. **12(4)** (2022) 617-638; http://dx.doi.org/10.5599/jese.1201

Open Access : : ISSN 1847-9286

https://pub.iapchem.org/ojs/index.php/JESE

Original scientific paper

Electrodeposition of strictly α,α'-polythiophene chains on oxidizable metals in acidic concentrated aqueous media

Mimouna Bouabdallaoui[1,✉], Zaynab Aouzal[1], Abdel Qader El Guerraf[1], Mohammed Bazzaoui[2] and El Arbi Bazzaoui[1]

[1]*Laboratory of Applied Chemistry and Environment, Faculty of Sciences, Mohammed First University, 60000 Oujda, Morocco*

[2]*Materials and Environmental Laboratory, Faculty of Sciences, Ibn Zohr University, 80000 Agadir, Morocco*

Corresponding author: ✉*mimounabouabdallaoui@gmail.com*

Received: December 3, 2021; Accepted: January 11, 2022; Published: January 19, 2022

Abstract

Electropolymerization of thiophene was performed in aqueous acidic media on various substrates, namely, titanium, nickel and SS steel. The films were successfully elaborated using voltamperometric, chronopotentiometric and chronoamperometric techniques. It was shown that concentrated acids increase the solubility of the monomer, lower its oxidation potential and inhibit the dissolution of the working electrode. Furthermore, the electrosynthesized polythiophene (PT) films are homogeneous and present similar properties to those obtained in organic media. On the other hand, analyses by X-ray photoelectron and infrared spectroscopies indicate the higher oxidation state of the polymers and the contribution of the supporting electrolyte in the doping process. In addition, IR spectra have demonstrated the strictly α, α' linked polythiophene chains and an estimated degree of polymerization (DP) of about 40. Finally, scanning electron microscopy (SEM) has been used to characterize the morphology of the obtained coating. In this context, the nature of the films depends closely on the type of the electrode, the electrosynthesized mode and the electrolytic medium.

Keywords

Electropolymerization; polythiophene, aqueous acidic media; oxidizable metals; vibrational and elemental analyses

Introduction

Polythiophene (PT) and its derivatives are very promising conducting polymers due to their numerous remarkable properties such as environmental and thermal stability [1-3], high electrical conductivity [4-6] and interesting electronic and optical characteristics [7-10]. Thanks to these features, polythiophene offers several industrial applications in various fields, including electronic

devices such as transistors [11-13], organic light-emitting diodes (OLEDs) [14,15], photovoltaic cells [16-19], electrochromic devices [20,21] and sensors [22-24].

Due to their high color intensity in the visible region and their strong dyeing power, PT and derivatives are often used as coloring matters. This interesting property makes these types of polymers ideal in solar cells and electrochromic devices, especially when a bright and intense color is required. As an example, we cite electrochromic materials based on the copolymerization of 3,4-ethylenedioxythiophene (EDOT) and naphthalene [25] or 1,4-bis(3-hexylthiophen-2-yl)benzene and EDOT [26]. Recently, transistors based on alternating copolymers of thiophene and thiadiazol have been reported. The material has shown an ambipolar behavior which is still rare [27].

Generally, polythiophene derivatives films are prepared by electrochemical polymerization of the corresponding monomer on noble metals such as platinum [28-30] and gold [31,32] or optically transparent electrodes like indium tin oxide (ITO) [33]. However, such electrodes are too expensive to suit larger-scale industrial applications. In this context, several attempts have been reported to prepare PT films on less noble metallic substrates (Iron, Zinc, Aluminum…) [34-37]. The major problem associated with these types of metals is related to the higher gap between their oxidation potential and the polymerization potential of thiophene. This difference provides a dissolution of the electrode before the formation of the polymer.

Unlike polypyrrole and polyaniline, PT is generally synthesized in organic media [34,35] due to the poor solubility of the monomer in conventional aqueous solutions. However, the preparation of polythiophene in organic solvents requires relatively high potentials, which could irreversibly damage the conjugated system due to an overoxidation of the polymer chains [38,39]. By adding bithiophene to thiophene solutions or converting thiophene to oligomers, the electropolymerization potential can be greatly reduced.

Several procedures have been proposed to prepare PT films in aqueous media. The use of an aqueous emulsion of thiophene containing 0.1 M $NaClO_4$ as the supporting electrolyte has led to a homogeneous PT deposit on a platinum electrode [40]. The surface of the electrode was previously treated by potential cyclic scanning between -0.25 and 1.15 V in an aqueous solution of 0.5 M H_2SO_4. The PT films obtained from this emulsion have shown different properties from those elaborated in organic medium. On the other hand, the electroplymerization of thiophene oligomers (terthiophene and tetrathiophene) in a highly concentrated phosphoric acid solution has been reported [41]. The electrosynthesis is generally carried out 24 hours after the thiophene addition to the acidic medium and, under these conditions, the solution turns yellow, indicating the formation of the oligomers. The use of the moderately concentrated perchloric acid (5 M) led to a significant decrease of the electropolymerization potential to about 0.9 V instead of 1.6 V/SCE [42].

In terms of solubility, the use of heteropolyacids ($H_3PW_{12}O_{40}$, $H_4SiW_{12}O_{40}$, $H_3PMo_{12}O_{40}$) promotes the electropolymerization of thiophene by the formation of a monomer-heteropolyanion complex soluble in water [43,44]. In addition, a micellar solution containing a surfactant like sodium dodecyl sulphate (SDS) could increase the solubility of thiophene and make electrosynthesis possible in aqueous media [30,37].

In a similar vein, the substitution of thiophene with groups such as alkylsulphonate increases its solubility in water [45]. However, it is important to emphasize that these substituents increase the oxidation potential of the monomer and affect the overall properties of the corresponding polymer. According to some published papers, the oxidation potential of thiophene monomers substituted by electron-withdrawing groups, such as 3-bromothiophene and 3-chlorothiophene, increases due to the

reduction of the electron density of the thiophene ring, which makes secondary reactions more likely during electropolymerization [46].

Recently, the electropolymerization of thiophene in ionic liquids based on quaternary phosphornium cations and a bis(fluorosulfonyl) amide anion on a platinum electrode has been described [47]. Room-temperature ionic liquids (RTILs) are low-melting organic compounds composed solely of ions. RTILs have unique physicochemical properties, such as relatively high ionic conductivity, very low volatility, high thermal stability and low flammability. Due to their properties, RTILs have been studied as promising electrolytic media for various electrochemical systems and devices [48,49]. In particular, RTILs based on quaternary phosphonium cations have relatively high conductivity and low viscosity in comparison with other RTILs [50-52]. By using such compounds in the preparation of PT films, homogeneous, thick and electroactive films have been obtained.

In this context, this paper will be devoted to studying the thiophene electropolymerization in two highly concentrated solutions, namely, phosphoric and perchloric acids. The synthesis will be achieved on various oxidizable metals that are titanium (Ti), nickel (Ni) and stainless steel (SS) by different electrosynthesis techniques. Finally, the structural, elemental and morphological analysis of the prepared coatings will be carried out to further discuss the effect of the supporting electrolyte on the doping level and surface topography.

Experimental

Thiophene (99 %, Aldrich) was purified by distillation under vacuum and stored under argon before use. Phosphoric (≥ 85 %) and perchloric (70 %) acids were obtained from Sigma-Aldrich and used as received.

The electrochemical experiments were performed in a one-compartment cell using an Origalys potentiostat/galvanostat monitored by Origamaster 5 software. The working electrode was an oxidizable metal disk: titanium (42.7 % Ti), nickel (60.3 % Ni) or SS steel (48.6 % Fe). The auxiliary electrode was a stainless-steel plate, and all potentials were measured vs. a saturated Ag/AgCl/Cl^- reference electrode.

XPS analysis was performed with a Vacuum Generators Escalab MKI spectrometer equipped with Mg Kα (1256.6 eV) and Al Kα (1486.6 eV) sources operating at 200 mW. Spectra were calibrated against the 1s carbon electron peak (285 eV binding energy) of the polythiophene ring carbon atoms as an internal reference.

Scanning electron micrographs of all samples were obtained using JOEL Ltd., JXA-8900 instrument. The pressure of the microscope chamber was maintained between 4 and 10 Pa.

The FTIR analysis was carried out using a Fourier transform infrared spectrophotometer model JASCO FT/IR-4200. The samples were finely ground with an anhydrous alkaline halide (KBr grade IR) and then compressed into pellets.

Results and discussion

Mechanism of oligomerization of thiophene in concentrated acids

Generally, thiophene is quite unstable in strongly acidic solvents and the synthesis in this media produces thiophene oligomers. In this context, many researchers have studied the polymerization of thiophene and derivatives (methylthiophene, butylthiophene…) in acidic media [53-55]. It has been found that concentrated orthophosphoric acid produces soluble thiophene oligomers composed mainly from trimers, smaller amounts of pentamers and traces of dimers [41].

A structural study by infrared spectroscopy of the formed trimer (2,4-di-(2-thienyl)-thiol) indicates the presence of both thiolane and thiophene rings [53]. On the other hand, the UV-visible-NIR optical analysis of the concentrated thiophene-acidic solutions (H_3PO_4 and $HClO_4$) reported in the literature indicated the formation of oligomers [41,42]. In the case of $HClO_4$, immediately after the addition of thiophene, a low absorption band at 307 nm characterizing the bithiophene is observed [42]. While in phosphoric acid, after four days, the thiophene band disappears and two bands at 350 and 400 nm attributed to terthiophene and tetrathiophene respectively appear [41,56].

Seymour *et al.* [53] have proposed a mechanism explaining the steps leading to the trimer formation. In Scheme 1, the first step consists of a proton addition to the α position of the thiophene ring, which leads to three resonance forms (A, B and C) of which only A and B can react.

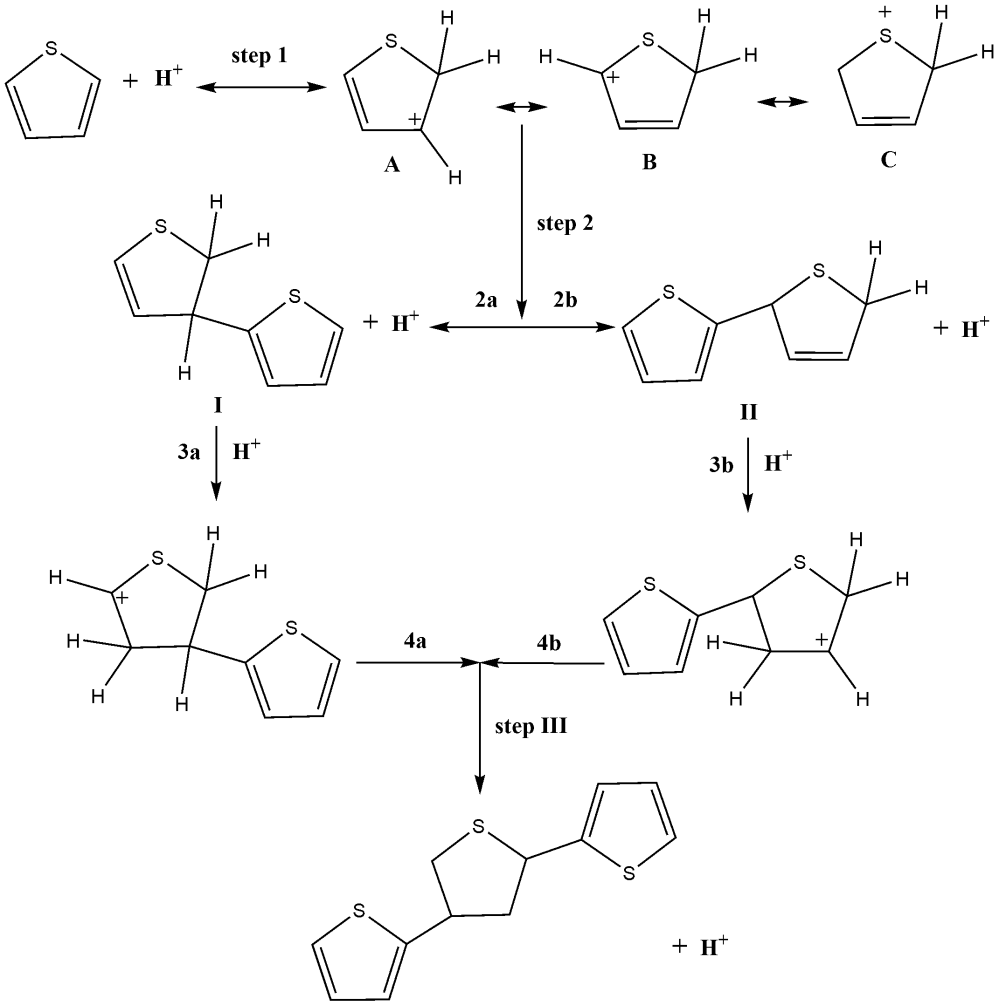

Scheme 1. *Mechanism explaining the formation of trimer in concentrated acid medium proposed by Seymour* et al. *[53]*

In A, there is an electron-deficient carbon in the position β that can attack the electron-rich α' position of form B with the expulsion of a proton to produce species I (step 2a). Step 3a involves the addition of a proton to a sulfur-olefin system. Step 4a, which gives the trimer, is similar to step 2a. and step 2b is the same as step 2a. In step 3b, it is possible to add a proton at position 3 or 4 of the thiolene ring system. If the proton was added to position 3, steric hindrance would tend to prevent thiophene from adding to position 4. However, the initial addition of a proton at position 4 would lead to the unhindered attack of thiophene at position 3. The final product, in this case, is still 2,4-di-(2-thienyl)-thiolane.

Electrochemical behavior of oxidizable metals in concentrated acidic media in the absence of monomer

Figure 1 shows the electrochemical behavior of SS, Ti, and Ni in the absence of thiophene in an aqueous medium of phosphoric acid 15 M H_3PO_4. In addition, for comparison purposes, platinum (Pt) inert electrode was also studied in the same conditions. By scanning the potential between 0 and 1.1 V. The voltammogram recorded on a platinum electrode, both mediums reflect the inert behavior of this metal classified as a noble metal due to its relatively high oxidation potential compared to other metals.

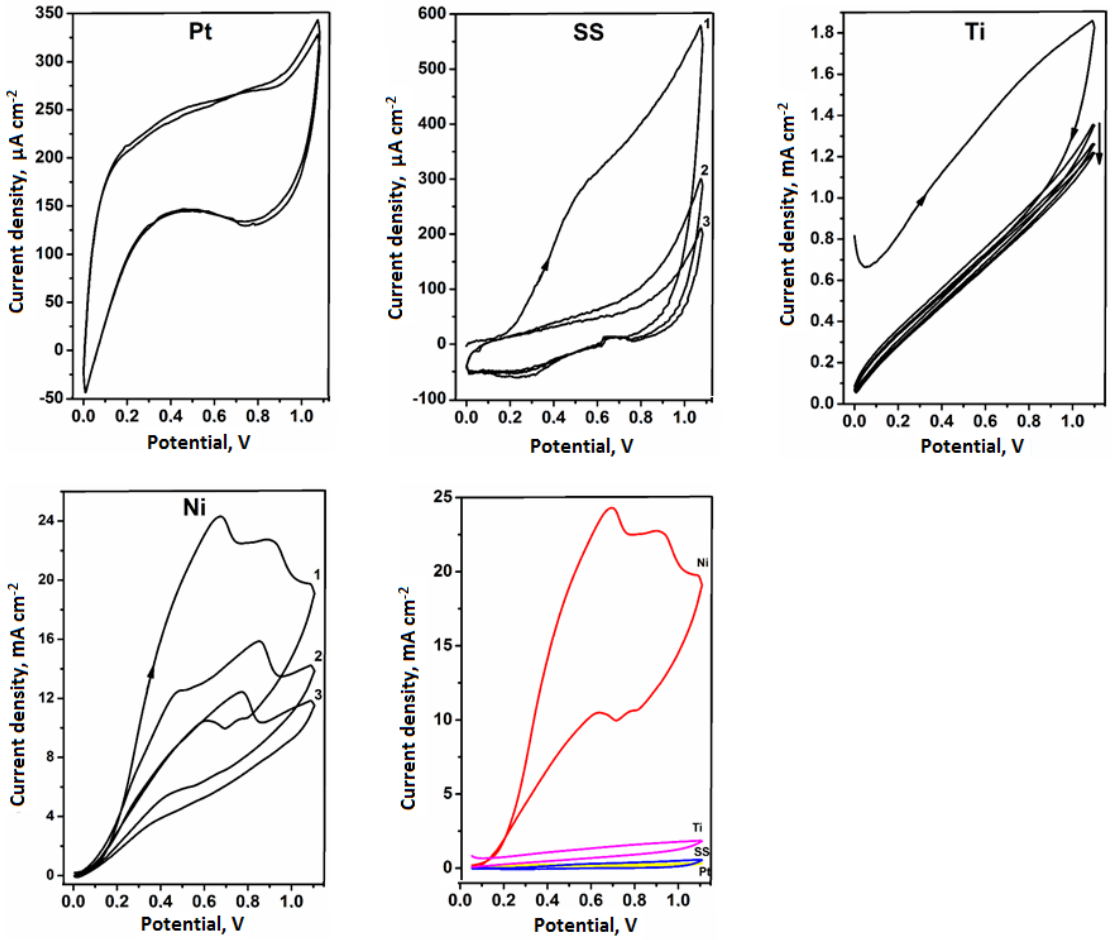

Figure 1. *Electrochemical behavior of metallic substrates in 15 M H_3PO_4 in the absence of thiophene. Scan rate 100 mV s^{-1}*

In 15 M H_3PO_4, in the case of SS substrate, the first scan shows a broad peak with a current density of about 600 µA cm^{-2} attributed to the oxidation of the metal. In the second cycle, the current decreases to 300 µA cm^{-2} under the effect of passivation, and the voltammogram becomes similar to those obtained on platinum.

In the case of Ti, during the first scan, the current increases to 1.8 mA cm^{-2} then decrease gradually during subsequent successive scans, which reflects the passivation of the metal in this medium. What characterizes this metal in its active state is the uniform formation of titanium dioxide (TiO_2) [57,58] which inhibits the dissolution of the electrode:

$$Ti + 2H_2O \rightarrow TiO_2 + 4H^+ + 4e^- \quad (1)$$

The formation of Ti_2O_3 can also occur [59], however, this unstable species, in contact with water, is rapidly oxidized to TiO_2:

$$Ti_2O_3 + H_2O \rightarrow 2TiO_2 + 2H^+ + 2e^- \quad (2)$$

The voltammogram obtained on nickel is more complex. It is composed of the superposition of at least two oxidation peaks. In the case of this metal, the current density reaches relatively high values (25 mA cm^{-2} during the first scan) and despite the drop in intensity observed during successive scans, the current remains significant in comparison with the other metals.

The dissolution of nickel in an acidic medium follows the reaction:

$$Ni + 2H_3O^+ \rightarrow Ni^{2+} + H_2 + 2H_2O \quad (3)$$

The nickel passivation reaction is:

$$Ni + 2H_2O \rightarrow NiO_2 + 4H^+ + 4e^- \quad (4)$$

Similar electrochemical behaviors were observed in concentrated perchloric acid 9 M $HClO_4$ (Figure 2). In the case of SS, a metal oxidation peak at 0.05 V was observed during the first cycle, followed by passivation during subsequent scans. The presence of this peak was also mentioned by Ahmad *et al.* [60] at -0.2 V *vs.* SCE during the passivation of an SS-430 plate by cyclic voltammetry between -0.4 and 1.1 V *vs.* SCE in 1 M H_2SO_4.

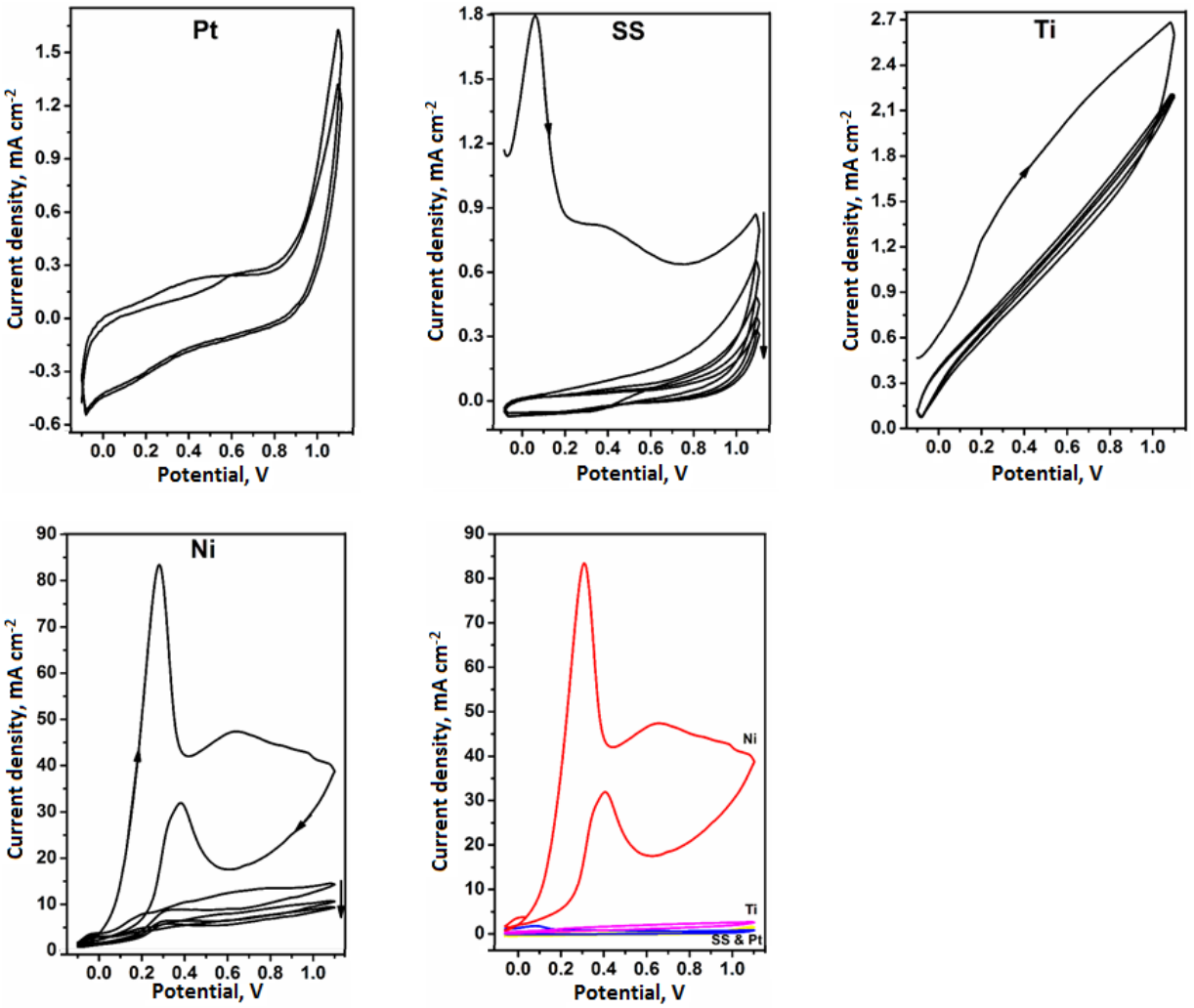

Figure 2. *Electrochemical behavior of metallic substrates in 9 M $HClO_4$ in the absence of thiophene. Scan rate 100 mV s^{-1}*

The titanium electrode also keeps the same behavior observed in H_3PO_4. Indeed, the first scan shows a wave linked to the oxidation of the metal, followed by passivation resulting from the decrease in the current during subsequent scans.

On the contrary, in the case of nickel, different behavior from that observed in H_3PO_4 is present when using $HClO_4$. The first scan shows an intense oxidation peak at 0.3 V, which reaches 83 mA cm^{-2} followed by a wide peak of lower intensity (48 mA cm^{-2}) at 0.65 V. At the return scan, a positive peak is observed on the anodic side at 0.38 V. This behavior is often attributed to the desorption of the passivation layer on the surface. These peaks disappear when the number of scans increases, and the current takes lower values (<10 mA cm^{-2}).

The perchlorate anion could be involved in the passivation phenomenon. Its reduction in chlorate ions follows the reaction [61,62]:

$$ClO_4^- + 2H^+ + 2e^- \rightarrow ClO_3^- + H_2O \quad (5)$$

The chlorate anion could also be reduced according to the following reaction:

$$ClO_3^- + 6H^+ + 6e^- \rightarrow Cl^- + 3H_2O \quad (6)$$

The product of the reduction reaction is chloride ion, according to the overall reaction:

$$ClO_4^- + 8H^+ + 2e^- \rightarrow Cl^- + 2H_2O \quad (7)$$

Electropolymerization of thiophene on various oxidizable metals

Cyclic voltammetry

Fig. 3 shows the potentiodynamic curves of the thiophene electropolymerization in 15 M H_3PO_4 medium on the surface of different oxidizable substrates. In the case of a platinum electrode, the first scan is characterized by an anodic peak at about 1 V, which indicates the oxidation of thiophene oligomers (terthiophene) [41,63] formed by chemical oligomerization in H_3PO_4. During the reverse scan, a large cathodic peak is observed at 0.1 V attributed to the reduction of the first layer of the polymer. The growth in the current density during successive potential scanning confirms the increase in the thickness of the conducting polymer deposited on the platinum surface.

In the case of stainless steel and titanium, the first potential scan reveals the presence of a wave generated from the oxidation of the metallic substrate. Afterward, the polymerization of the monomer begins at 0.9 V and the oxidation and reduction peaks of the polymers increases in intensity with the cycles. From the 2nd scan, the voltammogram becomes similar to those recorded on Pt.

Completely different behavior is observed in the case of nickel. During the first scan, we noticed an intense oxidation peak (11 mA cm^{-2}) which is generally attributed to the working electrode, followed by a passivation step where the current keeps a relatively low value (3 mA cm^{-2}). Although a couple of redox peaks of the polymer are not well-defined in the voltammogram, a thin and homogeneous black PT film is formed on the surface of the electrode.

The electropolymeization of thiophene was also achieved in perchloric acid 9 M $HClO_4$ (Fig. 4). For a platinum electrode, the increase in the current observed at 0.9 V corresponds to the oxidation of the oligomers, which leads to the formation of the polythiophene film. In this case, the anodic and cathodic peaks of the polymer are quite large in comparison with those recorded in phosphoric acid. This phenomenon is explained by the slow kinetics diffusion of the doping anions through the film. Otherwise, this characteristic has been linked to the processes of reorganization of the polymer chains, accompanying the expulsion or inclusion of the anions during the doping-dedoping process [14].

On SS, the same behavior is observed during successive potential cycling. However, in this case, a second redox couple of peaks appears in the voltammograms. The first pair at (0.3 V, 0.1 V) is that of the polymer, while the second at (0.7 V, 0.55 V) can be attributed to chains whose length is between those of the polymer and starting oligomers. This hypothesis is supported by the well-known fact that the oxidation potential increases when the length of the chain decreases and *vice versa*.

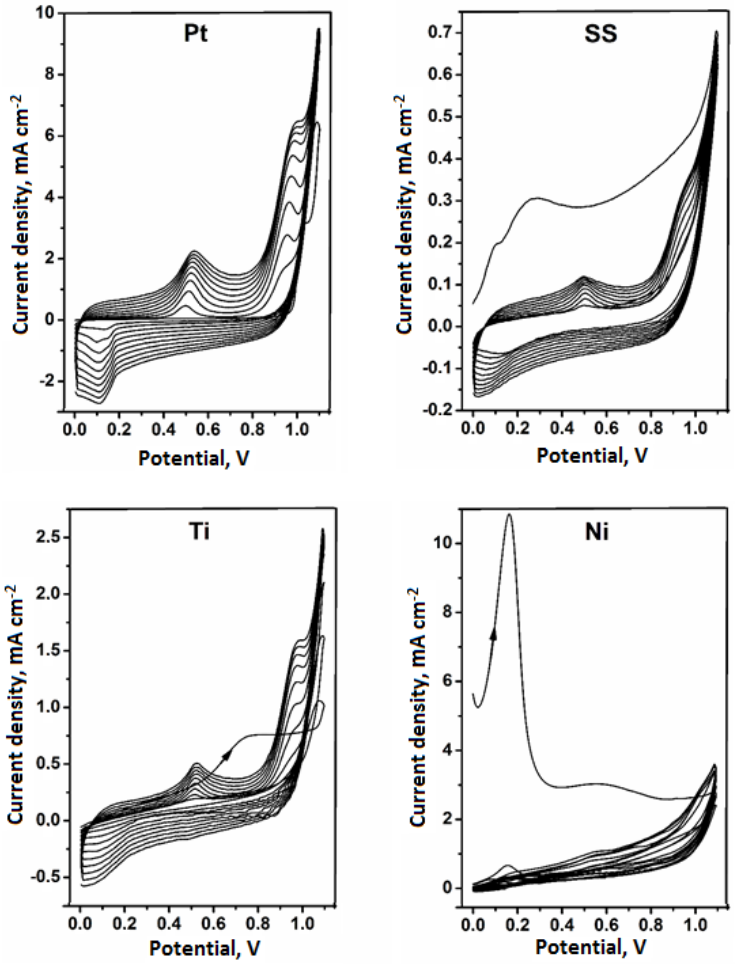

Figure 3. *Cyclic voltammograms of PT growth in H_3PO_4 15 M medium on various metallic substrates. Scan rate 100 mV s^{-1}*

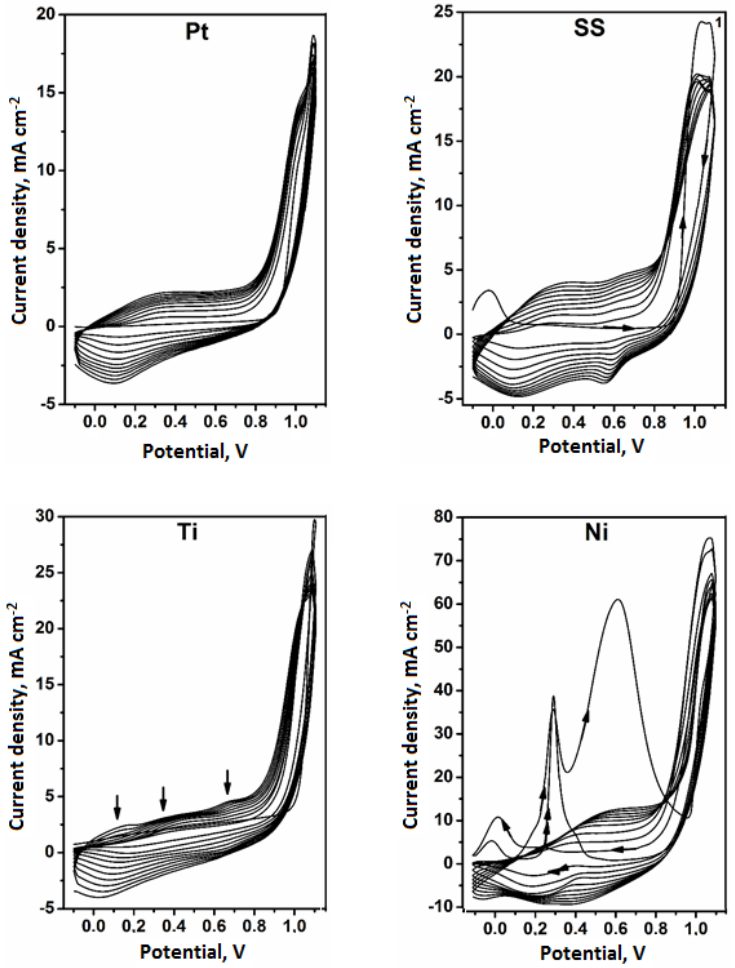

Figure 4. *Cyclic voltammograms of PT growth in 9M $HClO_4$ medium on various metallic substrates. Scan rate 100 mV s^{-1}*

In the case of nickel, the first scans reveal a preliminary stage of competition between the dissolution of the working electrode and the electropolymerization reaction. After three cycles, the electropolymerization process becomes preponderant and leads to the formation of a black PT film on the surface of the electrode. The voltammogram then takes a similar shape to the potentiodynamic curves recorded on Pt.

Galvanostatic technique

The thiophene electropolymerization was carried out galvanostatically by applying to the working electrode different current densities ranging between 0.1 and 10 mA cm^{-2}. As expected, the potential-time (*E* - *t*) curves vary considerably with the applied current densities (Figure 5 and Table 1).

When using a platinum electrode in both acidic media, an applied current density of 0.1 mA cm^{-2} is not sufficient for the formation of the polymer. Obtaining a homogeneous and adherent film of polythiophene on the surface requires a value of 1 mA cm^{-2}. For higher current densities (j > 1 mA cm^{-2}), the potential plateaux stabilize at values (Table 1) corresponding to the solvent oxidation according to the reaction [42]:

$$2H_2O \rightarrow O_2 + 4H^+ + 4e^- \quad (8)$$

Indeed, the working electrode is covered with a gaseous sheath, and the PT film formed on the surface undergoes a partial degradation.

In the case of SS, the growth of PT film in 15 M H_3PO_4 medium is observed from 1 mA cm^{-2}. Above 2.5 mA cm^{-2}, the decomposition of H_2O occurs and prevents the formation of PT on the surface of the electrode. For 9 M $HClO_4$, the homogeneity is observed only for applied current density higher than 2.5 mA cm^{-2}.

On a nickel plate and for both acidic media, the potential stabilizes at very low values when applying a current density between 0.1 and 2.5 mA cm^{-2} (Table 1). The formation of a homogeneous PT film requires the application of 5 mA cm^{-2}. At this current density, the galvanostatic curves show the competition between the electropolymerization reaction and the dissolution of the metallic substrate.

The use of titanium as the working electrode has shown a different behavior. In phosphoric acid, the potential keeps negative values at low current densities and increases drastically to very high values (> 2 V) when applying a current density of 5 mA cm^{-2}. In this case, no film is observed on the surface of the electrode. On the other hand, a homogeneous and thick PT coating could be obtained in an $HClO_4$ medium from 5 mA cm^{-2}.

Table 1. *Galvanostatic electropolymerization of thiophene in 15 M H_3PO_4 and 9 M $HClO_4$ on Pt, SS, Ni and Ti*

	Pt			SS			Ni			Ti		
j / mA cm^{-2}	E / V	F*	H**	E / V	F*	H**	E / V	F*	H**	E / V	F*	H**
Phosphoric acid												
0.1	0.7	-		1.10	-		-0.10	-		-0.4	-	
1.0	0.9	+	+	1.15	+	+	-0.10	-		-0.2	-	
2.5	1.6	+	-	1.18	+	+	-0.03	-		0.2	-	
5.0	2.3	+	-	1.27	+	-	1.56	+	+	2.5	-	
10	2.5	+	-	1.46	+	-	1.78	+	-	4.7	-	
Perchloric acid												
0.1	0.60	-		-0.10	-		-0.05	-		-0.48	-	
1.0	1.00	+	+	0.80	-		0.10	-		0.10	-	
2.5	1.75	+	-	0.94	+	+	0.20	-		0.23	-	
5.0	2.25	+	-	0.95	+	+	1.10	+	+	1.00	+	+
10.0				1.15	+	+	1.40	+	+	1.75	+	+

*F - formation, obtaining the PT film (+) or not (-); **H - homogeneity, good (+) or bad (-)

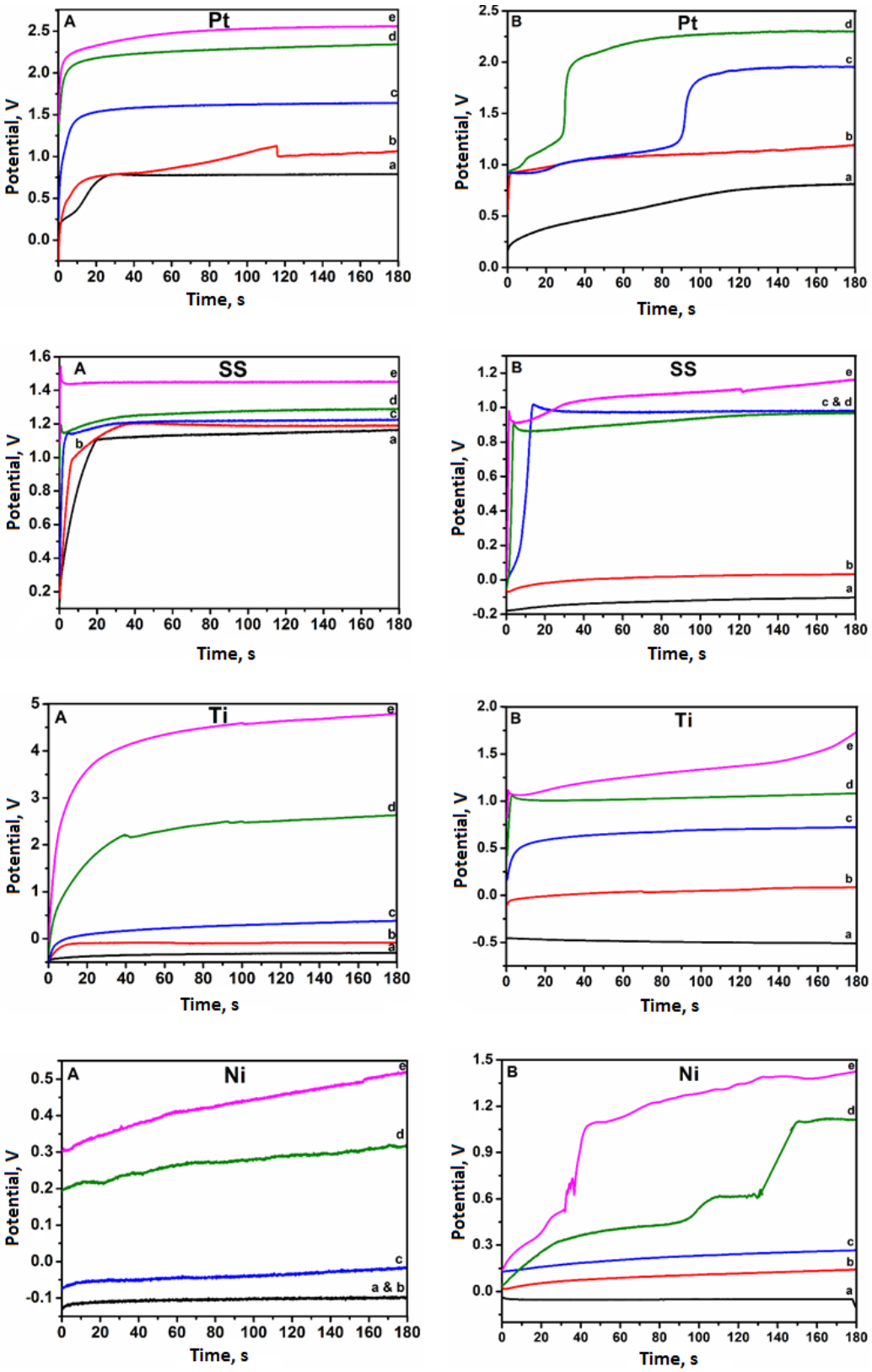

Figure 5. *Potential-time curves recorded during the galvanostatic electropolymerization of thiophene on various metallic substrates in (A) 15 M H_3PO_4 and (B) 9 M $HClO_4$. Applied current densities: a) 0.1; b) 1; c) 2.5; d) 5 and e) 10 mA cm^{-2}*

Potentiostatic technique

Likewise, the electrosynthesis of polythiophene can also be performed by the potentiostatic mode. Imposed potential values have been chosen in an interval from 0.7 to 1.2 V *vs.* Ag/AgCl that frames the known oxidation potential of the monomer (Figure 6).

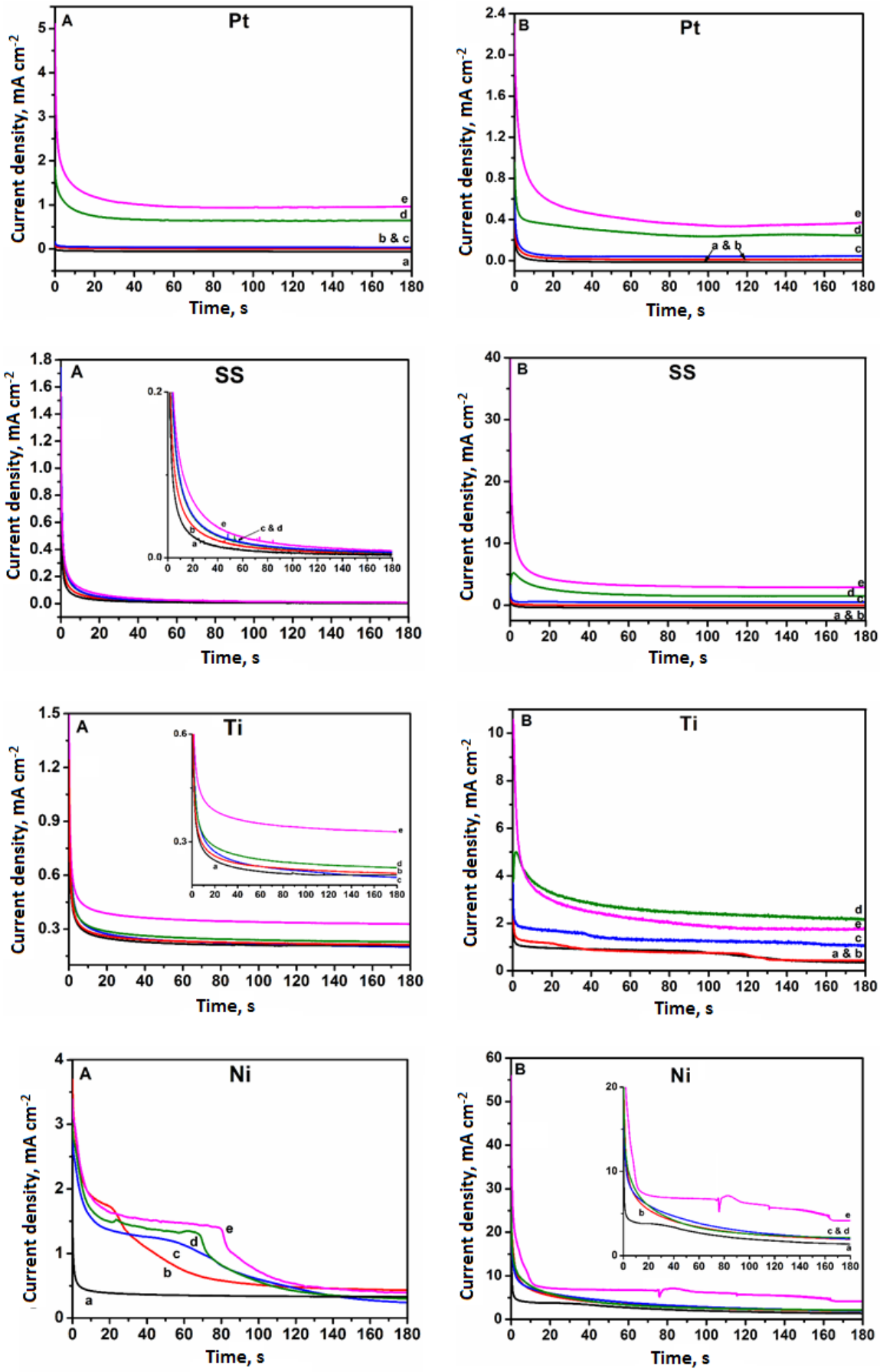

Figure 6. *Current density-time curves recorded during the potentiostatic electropolymerization of thiophene on various metallic substrates in (A) 15 M H_3PO_4 and (B) 9 M $HClO_4$. Applied potential: a) 0.7; b) 0.8; c) 0.9; d) 1 and e) 1.2 V vs. Ag/AgCl*

Table 2 describes the characteristic of the films (formation and homogeneity) with the applied potential. Generally, the threshold electropolymerization potentials are greater on oxidizable metals electrodes than those observed on Pt plates.

On the Pt electrode and for both acidic media, the electropolymerization occurs instantaneously at a potential value equal to or higher than 0.9 V versus Ag/AgCl. Homogeneous and adherent PT films are formed on the surface.

When the working electrode is a plate of SS, the threshold value of the potential that allows the electrodeposition of polythiophene films is 1 V versus Ag/AgCl. The increase of the value of the imposed potential on the WE provoked an increase of the plateau current density (*j* - *t*) and the thickness of the obtained coating.

In the case of nickel and titanium and while the thiophene electropolymerization takes place at a potential value equal or superior to 0.9 V in perchloric acid medium, it is necessary to apply a value at least equal to 1 V to form a deposit on the surface. For both cases, an applied potential of 1 V gives a homogenous film on Ni and Ti electrodes.

Table 2. *Potentiostatic electropolymerization of thiophene in 15 M* H_3PO_4 and 9 M $HClO_4$ on Pt, SS, Ni and Ti

E / V	Pt			SS			Ni			Ti		
	j / mA cm^{-2}	F*	H**	*j* / mA cm^{-2}	F*	H**	*j* / mA cm^{-2}	F*	H**	*j* / mA cm^{-2}	F*	H**
Phosphoric acid												
0.7	-0.1	-		0.01	-		0.5	-		0.24	-	
0.8	0.1	-		0.01	-		0.6	-		0.25	-	
0.9	0.2	+	+	0.02	-		0.4	-		0.26	-	
1	0.8	+	+	0.02	+	+	0.5	+	+	0.28	+	+
1.2	1.3	+	+	0.02	+	+	0.6	+	+	0.39	+	-
Perchloric acid												
0.7	-0.01	-		-0.1	-		0.2	-		0.6	-	
0.8	0.01	-		0.0	-		0.4	-		0.7	-	
0.9	0.03	+	+	1.1	-		0.4	+	-	1.5	+	-
1	0.30	+	+	3.9	+	+	0.4	+	+	2.0	+	+
1.2	0.50	+	+	4.9	+	+	0.6	+	+	2.8	+	+

*F - formation, obtaining the PT film (+) or not (-); **H - homogeneity, good (+) or bad (-)

Characterization of the polymeric coatings

After optimizing the experimental condition, the homogenous elaborated films were analyzed by several spectroscopic and microscopic techniques. This section aims to achieve a detailed quantitative analysis of the prepared coatings using X-ray photoelectron spectroscopy (XPS) and infrared vibrational spectroscopy (FTIR), as well as describing their morphology by scanning electron microscopy (SEM).

XPS analysis

Firstly, the elemental composition of the PT films electrodeposited on oxidizable metals in acidic media has been investigated by XPS.

The C 1s signal can be decomposed into four different components (Figure 7). The main peak at 285 eV corresponds to the C-C and C-H groups [31,42]. The second peak at 286.8 eV is attributed to the carbons that interact with the doping anion [31,42,64]. The third component of low intensity at 288.7 eV is associated with C-OH species [31,42] and the one at 290.5 eV, almost inactive, corresponds to the C=O carbonyl groups attached to the polymer chains as a result probably of some contamination [31,42].

The XPS analysis was also performed for reduced films. As shown in the figure, the peaks keep the same position and the change is noticed only in their intensity. Indeed, as presented in Table 3, there is a clear modification of the intensity ratios of each component compared to the total carbon intensity when reducing the PT film.

The significant decrease in the intensity ratio of $C_{286.8}$ / C_t strengthens the hypothesis described above related to the assignment of the peaks located at 286.8 eV. This latter is the signature of an interaction between the polymer and the doping anion. Hence, by reducing the PT film, a decrease in the intensity of this peak is expected.

Table 3. *The intensity ratios of different C 1s components compared to the total carbon intensity.*

			Peak intensity ratio			
			C_{285} / C_t	$C_{286.8}$ / C_t	$C_{288.7}$ / C_t	$C_{290.5}$ / C_t
H_3PO_4	Stainless steel	PT_{Ox}	0.73	0.19	0.05	0.03
		PT_{Re}	0.80	0.15	0.04	0.01
	Nickel	PT_{Ox}	0.44	0.39	0.09	0.08
		PT_{Re}	0.74	0.16	0.06	0.04
$HClO_4$	Stainless steel	PT_{Ox}	0.70	0.21	0.06	0.03
		PT_{Re}	0.79	0.15	0.04	0.02
	Nickel	PT_{Ox}	0.62	0.23	0.08	0.07
		PT_{Re}	0.76	0.16	0.05	0.03

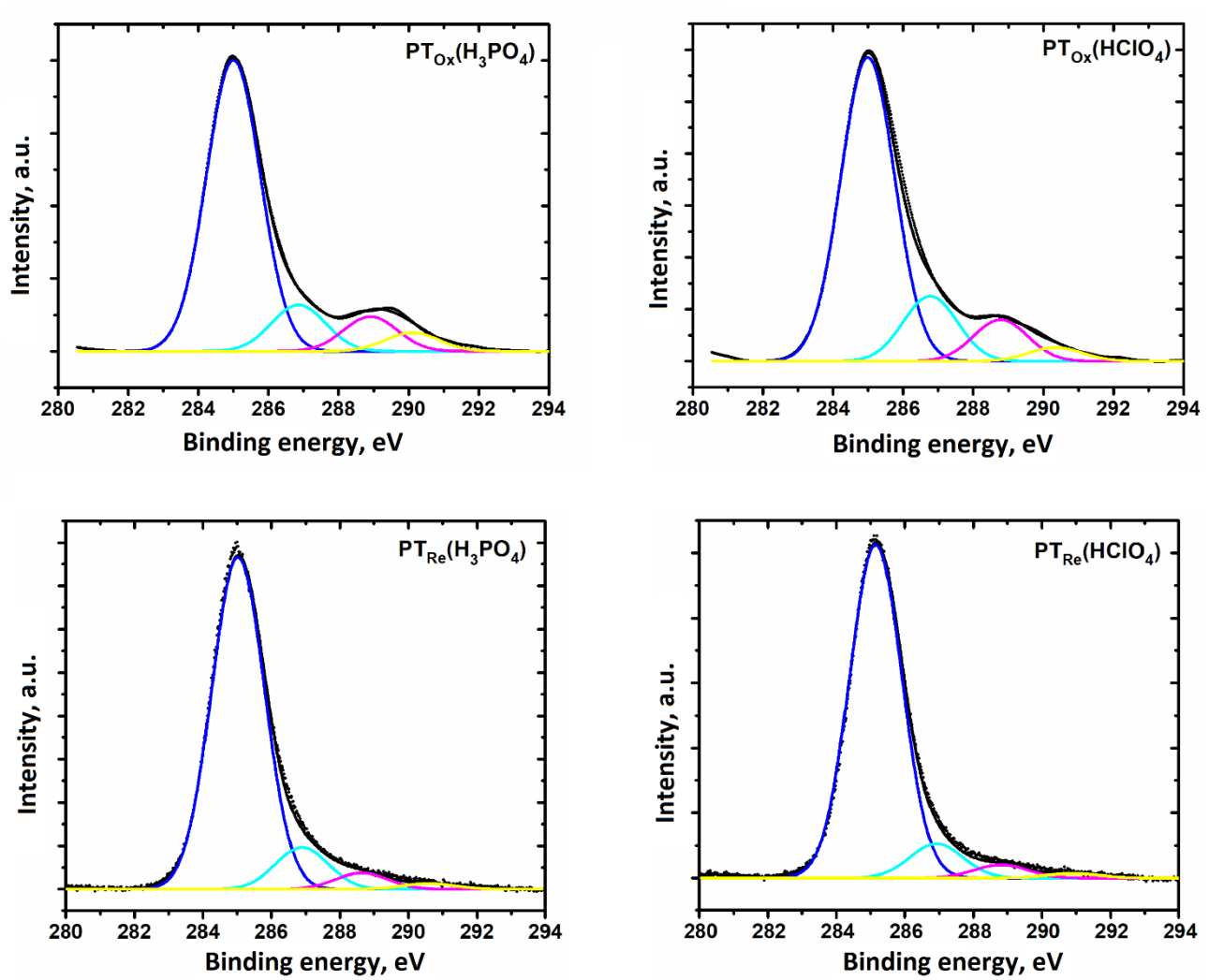

Figure 7. *C 1s XPS signal of doped and undoped PT films synthesized by potentiodynamic mode on SS in 9 M $HClO_4$ and 15 M H_3PO_4 acidic media*

The sulfur S 2p XPS signal contains two doublets (Figure 8), the first S_I located at (163.5 and 164.3 eV) and the second S_{II} at (165.1 and 166 eV), which are respectively associated with the neutral and oxidized sulfur atoms [31,42,64].

Regardless of the nature of the electrode, the intensity ratios S_{II}/S_t decrease from PT_{Ox} to PT_{Re} (Table 4). The second doublet S_{II} is more intense in the case of the doped film because of the positive charges introduced on the backbone of the polymer by oxidation.

The analysis of the Cl 2p XPS signal confirms the previous conclusions regarding the doping and dedoping of the polymer prepared in a perchloric acidic medium (Figure 8). In the oxidized state, two doublets are observed at (189 and 190.6 eV) and (198.3 and 200 eV). The first doublet Cl_I is assigned to chlorine atoms linked to the PT chains. The covalent bonds C-Cl are formed during the electropolymerization process, which requires a sweeping towards relatively high potential and causes an overoxidation of the polymer and the formation of chlorinated and oxygenated groups linked to the carbon skeleton [38]. This is in agreement with the peak C 1s at 286.8 eV [31,42].

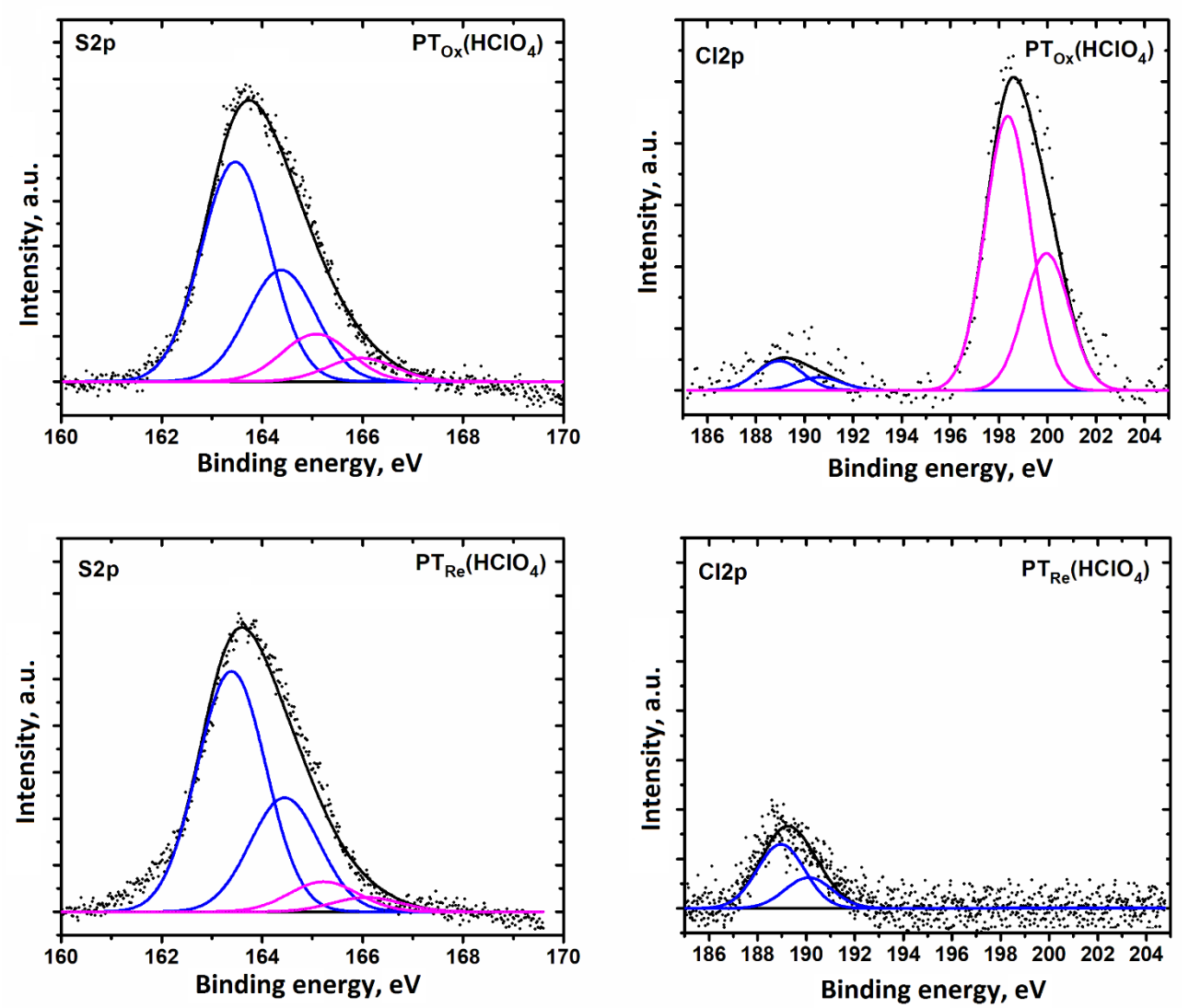

Figure 8. *S 2p and Cl 2p XPS signals of PT films synthesized by potentiodynamic mode in 9 M $HClO_4$ acidic medium on SS*

The second doublet Cl_{II} resulted from the presence of the perchlorate ion ClO_4^- as a doping species. After the reduction of the polythiophene films, this doublet disappears following the expulsion of the counter-ions.

Table 4. *The Intensity ratios of S_I and S_{II} components compared to the total sulfur intensity*

			Peak intensity ratio	
			S_I / S_t	S_{II} / S_t
$HClO_4$	Stainless steel	PT_{Ox}	0.74	0.26
		PT_{Re}	0.85	0.15
	Nickel	PT_{Ox}	0.72	0.28
		PT_{Re}	0.93	0.07

The intensity ratios of the two chlorine components compared to the chlorine and carbon signals decrease from the oxidized state to the reduced state (Table 5). Estimated doping rates based on I_{ClII} / I_{Ct} intensities ratio are ~15 to 20 % for oxidized films and between 0 and 1 % for reduced samples.

Table 5. *Intensity ratios of Cl_I and Cl_{II} components compared to the total chlorine intensity*

			Peak intensity ratio	
			Cl_I/Cl_t	Cl_{II}/Cl_t
$HClO_4$	Stainless steel	PT_{Ox}	0.29	0.71
		PT_{Re}	0.81	0.19
	Nickel	PT_{Ox}	0.32	0.68
		PT_{Re}	1.00	0.00

In the case of the film electrosynthesized in phosphoric acidic medium, the XPS analysis revealed the presence of the P 2p signal consisting of a single doublet at (134.3 and 135.3 eV) (Figure 9) attributed to the phosphorus of the doping anion PO_4^{3-} [65-68].

The spectra of the oxidized forms are more resolved and have a higher signal-to-noise ratio than those of the reduced state. The doping rate evaluated from the calculation of the intensity ratios of phosphorus and carbon gives overall values of approximately 0.22 (22 %) in the oxidized state and 0.02 (2 %) in the reduced state.

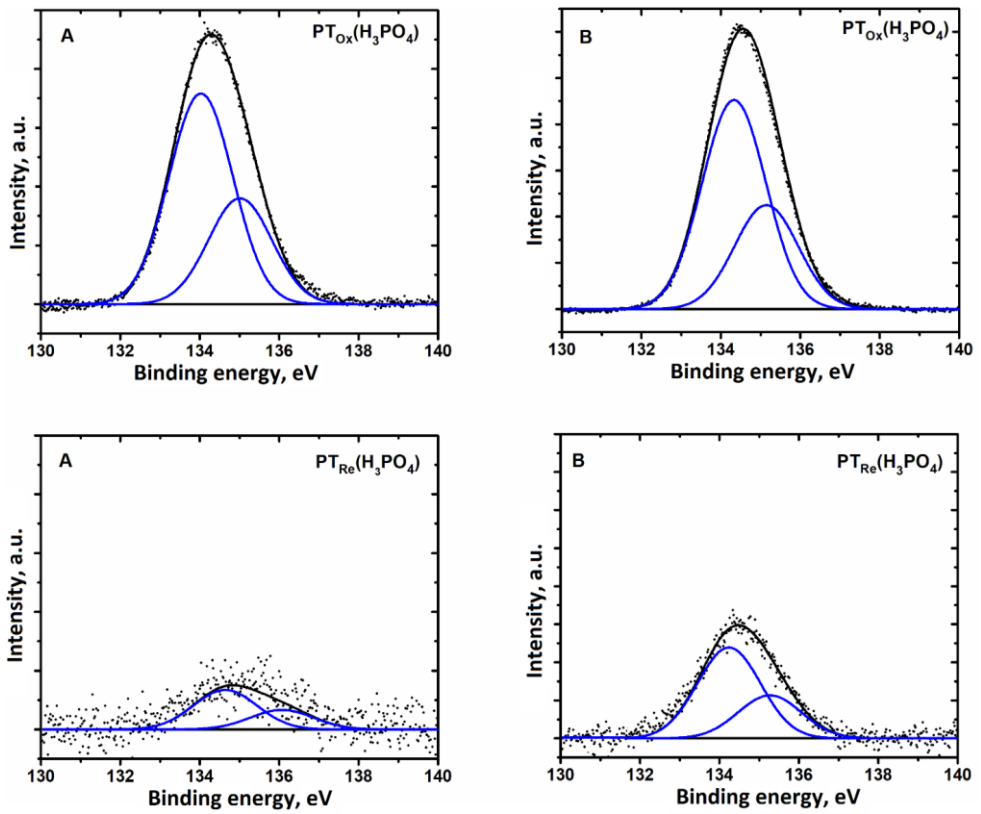

Figure 9. *P 2p XPS signal of PT films synthesized by potentiodynamic mode on (A) nickel and (B) stainless steel in 15 M H_3PO_4 acidic medium*

The XPS spectrum of oxygen O 1s (Figure 10) consists of the superposition of several contributions, including the doping anion, the residual water trapped in the polymeric matrix, the contamination by oxygen in the air, *etc.* Generally, the deconvolution of the O 1s XPS spectrum is difficult and requires a good knowledge of the sample to be analyzed. In our case, we have attempted the decomposition of the O 1s massif with three broad peaks and the result is satisfactory. The curve resulting from the deconvolution perfectly matches the raw signal. The peaks obtained are located at 531.7, 533.1 and 534.1 eV for the films synthesized in phosphoric acid and 529.5, 531.1 and 532.6 eV for the one prepared in perchloric acid. As mentioned above, these components whose relative intensities vary with the oxidation state of the polymer may have several origins: counter ion PO_4^{3-} and ClO_4^-, oxygenated groups such as carbonyls and sulfoxides attached to the polymer backbone, oxygen contamination and residual water.

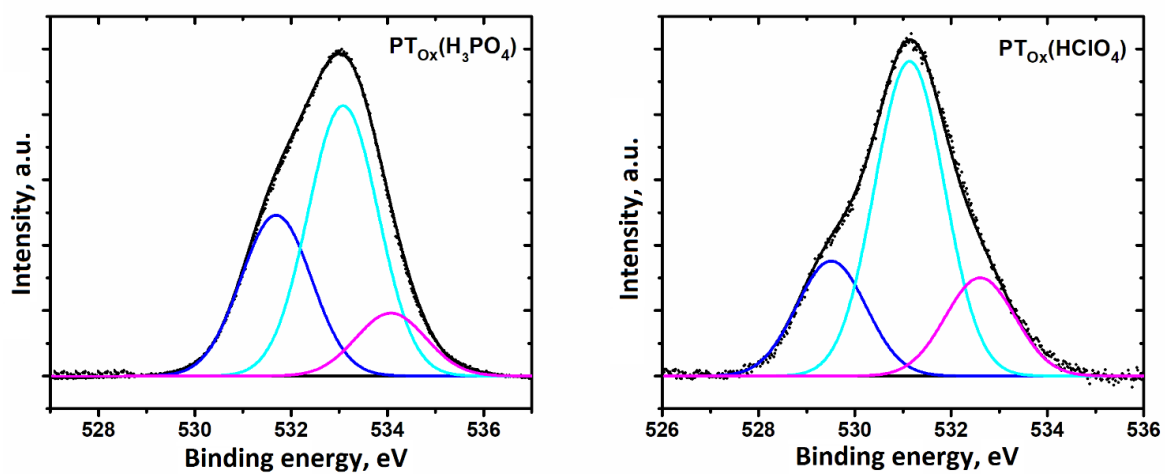

Figure 10. *O1s XPS signal of PT films synthesized by potentiodynamic mode on stainless steel in H_3PO_4 and $HClO_4$ acidic media*

FTIR analysis

PT films prepared in phosphoric and perchloric acidic media have been analyzed by infrared spectroscopy. The spectra are of good quality and all major bands are well defined (Figure 11).

The band at 1400 cm^{-1} characteristic of poly-2,5-thiophene confirms the α,α' coupling of thiophene rings, this observation is supported also by the absence of the tow bands at 820 and 730 cm^{-1} linked to the α,β' coupling [4,69]. The band situated at 1250 cm^{-1} is attributed to the C-C bonds of thiophene rings. The two peaks located at 1150 and 1170 cm^{-1} characterize the vibrations of the C-S bonds and two absorption bands at approximately 777 and 737 cm^{-1} belong to C-H aromatic bending vibrations.

The two bands at 1325 and 900 cm^{-1} are related to the vibrations of the PO_4^{3-} doping anion for PT films electrosynthesized in phosphoric acid [41,70] and the two others observed at 1090 and 625 cm^{-1} are attributed to the vibrations of the ClO_4^- counterion for the film elaborated in perchloric acid [42]. These bands confirm the conducting states of the elaborated coatings and their successful doping.

The degree of polymerization (DP) can be estimated from the relation of Furukawa *et al.* [4] and Sauvajol *et al.* [71]: DP = 2 [(R_0/R) + 2]. In this equation, R is the ratio of the out-of-plane vibrations modes of the C-H bonds in the position β of monosubstituted (701 cm^{-1}) and 2,5-disubstituted thiophenes (788 cm^{-1}). R_0 = 1.7 is the value of R for α,α'-sexithiophene [4]. The average DP obtained is about 40; low value but very similar to those reported in the literature for polythiophene synthesized in an aqueous medium [42].

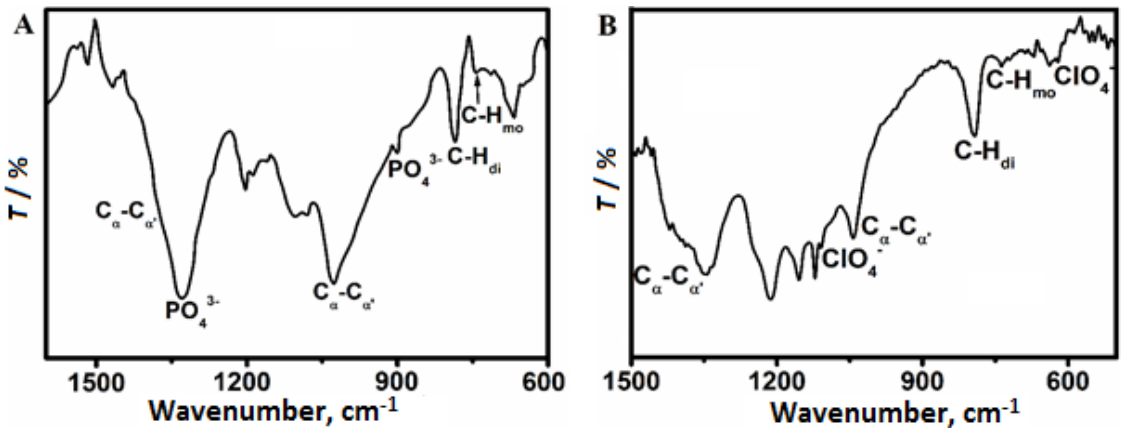

Figure 11. *FTIR spectra of PT films synthesized by potentiodynamic mode on stainless steel in 15 M H_3PO_4 (A) and 9 M $HClO_4$ (B)*

Morphology of PT films

To characterize the morphology of the prepared coatings, analysis by scanning electron microscopy (SEM) was also achieved in our study. The SEM micrographs presented in Figure 12 demonstrate the effect of the electrolytic medium, the nature of the electrode as well as the electrosynthesis technique on the topography of the obtained PT films.

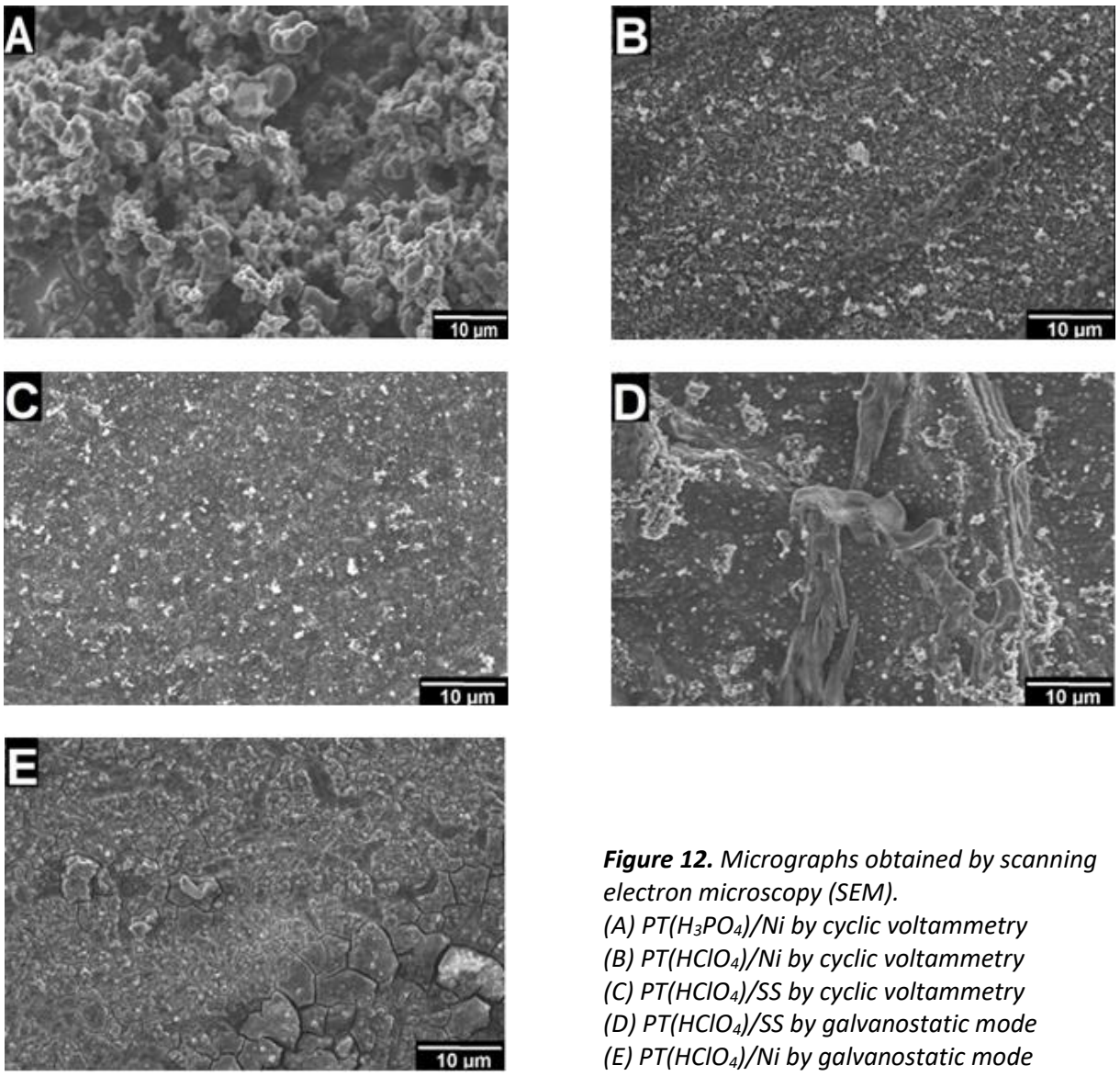

Figure 12. *Micrographs obtained by scanning electron microscopy (SEM).*
(A) PT(H_3PO_4)/Ni by cyclic voltammetry
(B) PT($HClO_4$)/Ni by cyclic voltammetry
(C) PT($HClO_4$)/SS by cyclic voltammetry
(D) PT($HClO_4$)/SS by galvanostatic mode
(E) PT($HClO_4$)/Ni by galvanostatic mode

In the case of nickel (Figure 12A, 12B and 12E), the polythiophene electrodeposited by cyclic voltammetry (20 cycles, v = 20 mV s^{-1}) in phosphoric acid (A), has a cauliflower structure with globules of about 1.5 µm. The film deposited under the same conditions in 9 M $HClO_4$ medium (Figure 12 B), has practically the same morphology. It presents a compact structure with different size particles. On the other hand, the film (Figure 12E) obtained by the galvanostatic mode (2 mA cm^{-2} for 10 min) shows a homogenous structure constituted by microspherical grains with some crack on its surface.

Scanning electron micrographs observed for a SS electrode are presented in Figures 12C and 12D. The film prepared in perchloric acid using cyclic voltammetry (Figure 12C) has the same morphology as the one synthesized with the same electrochemical method on Ni plates (Figure 12B). However, the external structure of the PT coating obtained under a constant current density (Figure 12D) appears with more defects on the surface. The globular structure is always maintained, but the homogeneity is better in the case of the film electrosynthesized by cyclic voltammetry.

Conclusions

In the present work, the electropolymerization of thiophene on stainless steel, nickel and titanium was successfully achieved in two different acidified aqueous media, phosphoric acid and perchloric acid.

As the electrodeposition of PT is generally realized on inert electrodes such as platinum in only organic media, the approach carried out in our study allowed us to overcome several problems related to the electropolymerization of thiophene on oxidizable metals in aqueous electrolytic media.

The procedure consists of producing soluble oligomers of thiophene by chemical oligomerrization in strongly acidic solvents. These oligomers, with mainly short chains, have a lower oxidation potential than the monomer. This allowed us to perform the electropolymerization at a much lower potential than thiophene (1 V instead of 1.6 V) and to avoid the oxidation of the water, which occurs at 1.23 V.

A preliminary study of the electrochemical behaviors of the oxidizable metals in the absence of the monomer revealed a passivation effect of the surface of the working electrodes. Since the oxidation reaction of the metallic substrates is inhibited, the addition of the monomer to the acidified electrolytic media has led to the electrodeposition of PT films. These coatings generally have the same structure and chemical composition as those usually produced in organic media on noble metals.

Infrared analysis has proved that the coupling mode in these films is an α,α' type with a degree of polymerization of approximately 40, comparable to that of the films deposited in the same media on Pt. Characterization by XPS spectroscopy confirmed the insertion of ClO_4^- and PO_4^{3-} as doping species in the matrix of the oxidized polymer. In this context, doping rates of approximately 20 % were calculated for both electrolytic media. In addition, surface analysis by SEM microscopy has demonstrated that the morphology of the polymer is closely dependent on the composition of the electrolytic medium, the nature of the metallic surface and the electrochemical synthesis technique. In this context, PT films generally present a globular structure with particles of different sizes.

Acknowledgements: *This work was supported by the MESRSFC and CNRST (Morocco) under grant No. PPR/30/2015.*

References

[1] R. L. Elsenbaumer, K. Y. Jen, G. G. Miller, L. W. Shacklette, *Synthetic Metals* **18(1-3)** (1987) 277-282. https://doi.org/10.1016/0379-6779(87)90892-7

[2] S. Lee, D. C. Borrelli, W. J. Jo, A. S. Reed, K. K. Gleason, *Advanced Materials Interfaces* **5(9)** (2018) 1701513. https://doi.org/10.1002/admi.201701513
[3] S. Iqbal, H. Khatoon, R. K. Kotnala, S. Ahmad, *Journal of Materials Science* **55(33)** (2020) 15894-15907. https://doi.org/10.1007/s10853-020-05134-z
[4] Y. Furukawa, M. Akimoto, I. Harada, *Synthetic Metals* **18(1-3)** (1987) 151-156. https://doi.org/10.1016/0379-6779(87)90870-8
[5] R. Kroon, D. Kiefer, D. Stegerer, L. Yu, M. Sommer, C. Müller, *Advanced Materials* **29(24)** (2017) 1700930. https://doi.org/10.1002/adma.201700930
[6] G. Cao, H. Cui, L. Wang, T. Wang, Y. Tian, *ACS Applied Electronic Materials* **2(9)** (2020) 2750-2759. https://doi.org/10.1021/acsaelm.0c00457
[7] J. W. Van der Horst, P. A. Bobbert, M. A. J. Michels, G. Brocks, P. J. Kelly, *Physical Review Letters* **83(21)** (1999) 4413-4416. https://doi.org/10.1103/PhysRevLett.83.4413
[8] A. Portone, L. Ganzer, F. Branchi, R. Ramos, M. J. Caldas, D. Pisignano, *Scientific Reports* **9(1)** (2019) 1-10. https://doi.org/10.1038/s41598-019-43719-0
[9] J. Kerfoot, S. A. Svatek, V. V. Korolkov, T. Taniguchi, K. Watanabe, E. Antolin, P. H. Beton, *ACS Nano* **14(10)** (2020) 13886-13893. https://doi.org/10.1021/acsnano.0c06280
[10] R. Schaffrinna, M. Schwager, *Materials Research Innovations* **25(1)** (2021) 23-28. https://doi.org/10.1080/14328917.2020.1728485
[11] H. Sirringhaus, P. J. Brown, R. H. Friend, M. M. Nielsen, K. Bechgaard, B. M. W. Langeveld-Voss, A. J. H. Spiering, R. A. J. Janssen, E. W. Meijer, P. Herwig, D. M. De Leeuw, *Nature* **401(6754)** (1999) 685-688. https://doi.org/10.1038/44359
[12] R. B. Ambade, S. B. Ambade, N. K. Shrestha, R. R. Salunkhe, W. Lee, S. S. Bagde, J. H. Kim, F. J. Stadler, Y. Yamauchi, S. H. Lee, *Journal of Materials Chemistry A* **5(1)** (2017) 172-180. https://doi.org/10.1039/c6ta08038c
[13] Z. F. Yao, J. Y. Wang, J. Pei, *Chemical Science* **12(4)** (2021) 1193-1205. https://doi.org/10.1039/d0sc06497a
[14] M. A. Ramírez-Gómez, K. K. Guzmán-Rabadán, E. Gonzalez-Juarez, M. Güizado-Rodríguez, G. Ramos-Ortiz, J. E. Alba-Rosales, H. Panzo-Medrano, V. Barba, M. Rodríguez, J. L. Maldonado, M. Á. Basurto-Pensado, *International Journal of Polymer Science* **2017** (2017) 1918602. https://doi.org/10.1155/2017/1918602
[15] P. J. Sephra, P. Baraneedharan, A. Arulraj, *Nanoelectronics devices (field-effect transistors, electrochromic devices, light-emitting diodes, dielectrics, neurotransmitters)* in *Advances in Hybrid Conducting Polymer Technology,* S. Shahabuddin, A. K. Pandey, M. Khalid, P. Jagadish, Eds.. Springer Nature, Switzerland; 2021. pp. 77-100. ISBN 978-3-030-62090-5
[16] S. Glenis, G. Horowitz, G. Tourillon, F. Garnier, *Thin Solid Films* **111** (1984) 93-103. https://doi.org/10.1016/0040-6090(84)90478-4
[17] Y. Kim, *Nat. Mater.* **5** (2006) 197-203. https://doi.org/10.1038/nmat1574
[18] S. Y. Kim, K. H. Lee, B. D. Chin, J.W. Yu, *Sol. Solar Energy Materials and Solar Cells* **93(1)** (2009) 129-135. https://doi.org/10.1016/j.solmat.2008.09.005
[19] P. Kumar, K. Ranjith, S. Gupta, P. C. Ramamurthy, *Electrochimica Acta*, **56(24)** (2011) 8184-8191. https://doi.org/10.1016/J.ELECTACTA.2011.06.114
[20] K. Kaneto, K. Yoshino, Y. Inuishi, *Japanese Journal of Applied Physics* **22(7)** (1983) L412-L414. https://doi.org/10.1143/JJAP.22.L412
[21] T. A. Welsh, E. R. Draper, *RSC Advance* **11(9)** (2021) 5245-5264. https://doi.org/10.1039/D0RA10346B
[22] A. S. Rad, *Journal of Molecular Modeling* **21(11)** (2015) 285. https://doi.org/10.1007/s00894-015-2832-9

[23] X. Wang, Y. Zheng, L. Xu, *Sensors Actuators, B Chem.* **255** (2018) 2952-2958. https://doi.org/10.1016/j.snb.2017.09.116
[24] B. H. Barboza, O. P. Gomes, A. Batagin-Neto, *Journal of Molecular Modeling* **27(1)** 20211-13. https://doi.org/10.1007/s00894-020-04632-w
[25] Y. Tao, H. Cheng, Z. Zhang, X. Xu, Y. Zhou, *Journal of Electroanalytical Chemistry* **689** (2013) 142-148. https://doi.org/10.1016/j.jelechem.2012.10.033
[26] C. Zhang, C. Hua, G. Wang, M. Ouyang, C. Ma, *Journal of Electroanalytical Chemistry* **645(1)** (2010) 50-57. https://doi.org/10.1016/j.jelechem.2010.04.009
[27] T. Yamamoto, T. Yasuda, Y. Sakai, S. Aramaki, *Macromolecular Rapid Communications* **26(15)** (2005) 1214-1217. https://doi.org/10.1002/marc.200500276
[28] E. A. Bazzaoui, G. Lévi, S. Aeiyach, J. Aubard, J. P. Marsault, P. C. Lacaze, *J. Phys. Chem.* **99(17)** (1995) 6628-6634. https://doi.org/10.1021/j100017a052
[29] M. A. del Valle, P. Cury, R. Schrebler, *Electrochimica Acta* **48(4)** (2002) 397-405. https://doi.org/10.1016/S0013-4686(02)00685-0
[30] N. Sakmeche, E. A. Bazzaoui, M. Fall, S. Aeiyach, M. Jouini, J. C. Lacroix, J. J. Aaron, P. C. Lacaze, *Synthetic Metals* **84(1-3)** (1997) 191-192. https://doi.org/10.1016/s0379-6779(97)80708-4
[31] E. A. Bazzaoui, M. Bazzaoui, J. Aubard, J. S. Lomas, N. Félidj, G. Lévi, *Synthetic Metals* **123(2)** (2001) 299-309. https://doi.org/10.1016/S0379-6779(01)00299-5
[32] A. R. Hillman, E. F. Mallen, *Journal of Electroanalytical Chemistry* **220(2)** (1987) 351-367. https://doi.org/10.1016/0022-0728(87)85121-5
[33] E. A. Bazzaoui, J. P. Marsault, S. Aeiyach, P. C. Lacaze, *Synthetic Metals* **66(3)** (1994) 217-224. https://doi.org/10.1016/0379-6779(94)90070-1
[34] M. Bazzaoui, E. A. Bazzaoui, J. I. Martins, L. Martins, *Materials Science Forum*, **455** (2004) 484-488. https://doi.org/10.4028/www.scientific.net/MSF.455-456.484
[35] S. Aeiyach, E. A. Bazzaoui, P. C. Lacaze, *Journal of Electroanalytical Chemistry* **434(1-2)** (1997) 153-162. https://doi.org/10.1016/S0022-0728(97)00044-2
[36] E. A. Bazzaoui, J. Aubard, N. Félidj, G. Laurent, G. Lévi, *Journal of Raman Spectroscopy* **36(8)** (2005) 817-823. https://doi.org/10.1002/jrs.1368
[37] E. A. Bazzaoui, S. Aeiyach, P. C. Lacaze, *Synthetic Metals* **83(2)** (1996) 159-165. https://doi.org/10.1016/S0379-6779(97)80070-7
[38] M. Bouabdallaoui, Z. Aouzal, S. B. Jadi, A. El Jaouhari, M. Bazzaoui, G. Lévi, E. A. Bazzaoui, *J. Solid State Electrochemistry* **21(12)** (2017) 3519-3532. https://doi.org/10.1007/s10008-017-3698-9
[39] M. Bouabdallaoui, Z. Aouzal, A. El Guerraf, S. B. Jadi, M. Bazzaoui, R. Wang, E. A. Bazzaoui, *Materials Today: Proceedings* **31** (2020) S69-S74. https://doi.org/10.1016/j.matpr.2020.06.067
[40] A. Czerwinski, H. Zimmer, C. Van Pham, J. Harry B. Mark, *Journal of The Electrochemical Society* **132(11)** (1985) 2669-2672. https://doi.org/10.1149/1.2113645
[41] S. Dong, W. Zhang, *Synthetic Metals* **30(3)** (1989) 359-369. https://doi.org/10.1016/0379-6779(89)90659-0
[42] E. A. Bazzaoui, S. Aeiyach, P. C. Lacaze, *Journal of Electroanalytical Chemistry* **364(1-2)** (1994) 63-69. https://doi.org/10.1016/0022-0728(93)02910-A
[43] M. Lapkowski, G. Bidan, M. Fournier, *Synthetic Metals* **41(1-2)** (1991) 407-410. https://doi.org/10.1016/0379-6779(91)91094-Q
[44] G. Bidan, E. M. Geniés, M. Lapkowski, *Synthetic Metals* **31(3)** (1989) 327-334. https://doi.org/10.1016/0379-6779(89)90800-X
[45] R. J. Walkman, F. Diaz, J. Bargon, *Journal of Physical Chemistry* **88(19)** (1984) 4343-4346. https://doi.org/10.1021/j150663a030

[46] S. Alkan, C. A. Cutler, J. R. Reynolds, *Advanced Functional Materials* **13(4)** (2003) 331-336. https://doi.org/10.1002/adfm.200304307
[47] K. Nishihata, K. Tsunashima, Y. Ono, M. Matsumiya, *ECS Transactions* **75(52)** (2017) 99-103. https://doi.org/10.1149/07552.0099ecst
[48] D. R. Macfarlane, M. Forsyth, P. C. Howlett, J. M. Pringle, J. Sun, G. Annat, W. Neil, E. I. Izgorodina, *Acc. Chem. Res*. **40(11)** (2007) 1165-1173. https://doi.org/10.1021/ef00049a003
[49] M. Armand, F. Endres, D. R. MacFarlane, H. Ohno, B. Scrosati, *Materials for Sustainable Energy* **8** (2010) 129-137. https://doi.org/10.1142/9789814317665_0020
[50] K. Tsunashima, M. Sugiya, *Electrochemistry Communications* **9(9)** (2007) 2353-2358. https://doi.org/10.1016/j.elecom.2007.07.003
[51] K. Tsunashima, M. Sugiya, *Electrochemistry* **75(9)** (2007) 734-736. https://doi.org/10.5796/electrochemistry.75.734
[52] K. Tsunashima, A. Kawabata, M. Matsumiya, S. Kodama, R. Enomoto, M. Sugiya, Y. Kunugi, *Electrochemistry Communications* **13(2)** (2011) 178-181. https://doi.org/10.1016/j.elecom.2010.12.007
[53] S. L. Meisel, G. C. Johnson, H. D. Hartough, *Journal of the American Chemical Society* **72(5)** (1950) 1910-1912. https://doi.org/10.1021/ja01161a015
[54] J. Wristers, *Journal of the American Chemical Society* **99(15)** (1977) 5051-5055. https://doi.org/10.1021/ja00457a026
[55] H. D. Hartough, J. W. Schick, J. J. Dickert Jr, *Journal of the American Chemical Society* ***72*(4)** (1950) 1572-1577. https://doi.org/10.1021/ja01160a040
[56] D. Margosian, P. Kovacic, *Journal of Polymer Science* **17(11)** (1979) 3695-3703. https://doi.org/10.1002/pol.1979.170171125
[57] D. J. Blackwood, L. M. Peter, *Electrochimica Acta* **34(11)** (1989) 1505-1511. https://doi.org/10.1016/0013-4686(89)87033-1
[58] C. P. De Pauli, M. C. Giordano, J. O. Zerbino, *Electrochimica Acta* **28(12)** (1983) 1781-1788. https://doi.org/10.1016/0013-4686(83)87014-5
[59] C. E. B. Marino, E. M. de Oliviera, R. C. Rocha-Filho, S. R. Biaggio, *Corrosion Science* **43(8)** (2001) 1465-1476. https://doi.org/10.1016/S0010-938X(00)00162-1
[60] N. Ahmad, A. G. MacDiarmid, *Synthetic Metals* **78(2)** (1996) 103-110. https://doi.org/10.1016/0379-6779(96)80109-3
[61] M. Y. Rusanova, P. Polaskova, M. Muzikar, W. R. Fawcett, *Electrochimica Acta* **51(15)** (2006) 3097-3001. https://doi.org/10.1016/j.electacta.2005.08.044
[62] G. Horányi, I. Bakos, *Journal of Electroanalytical Chemistry* **331(1-2)** (1992) 727-737. https://doi.org/10.1016/0022-0728(92)85002-K
[63] A. F. Diaz, J. Crowley, J. Bargon, G. P. Gardini, J. B. Torrance, *Journal of Electroanalytical Chemistry* **121** (1981) 355-361. https://doi.org/10.1016/S0022-0728(81)80592-X
[64] G. Morea, L. Sabbatini, R. H. West, J. C. Vickerman, *Surface and Interface Analysis* **18(6)** (1992) 421-429. https://doi.org/10.1002/sia.740180609
[65] D. Zhao, *Journal of Physical Chemistry C* **112(15)** (2008) 5993-6001. https://doi.org/10.1021/jp712049c
[66] M. J. Ariza, E. Rodríguez-Castellón, R. Rico, J. Benavente, M. Muñoz, M. Oleinikova, *Journal of Colloid and Interface Science* **226(1)** (2000) 151-158. https://doi.org/10.1006/jcis.2000.6805
[67] I. F. Amaral, P. L. Granja, M. A. Barbosa, *Journal of Biomaterials Science, Polymer Edition* **16(12)** (2005) 1575-1593. https://doi.org/10.1163/156856205774576736
[68] K. Rokosz, T. Hryniewicz, D. Matýsek, S. Raaen, J. Valíček, Ł. Dudek, M. Harničárová, *Materials (Basel)* **318(9)** (2016) 9-16. https://doi.org/10.3390/ma9050318
[69] S. Tanaka, M. Sato, K. Kaeriyama, *Die Makromolekulare Chemie* **185(7)** (1984) 1295-1306. https://onlinelibrary.wiley.com/doi/abs/10.1002/macp.1984.021850703

[70] F. A. Miller, C. H. Wilkins, *Analytical Chemistry* **24(8)** (1952) 1253-1294. https://doi.org/10.1021/ac60068a007

[71] J. L. Sauvajol, D. Chenouni, J. P. Lère-Porte, C. Chorro, B. Moukala, J. Petrissans, *Synthetic Metals* **38(1)** (1990) 1-12. https://doi.org/10.1016/0379-6779(90)90063-Q